International Journal of Steel Structures
December 2011, Vol 11, No 4, 467-479
DOI 10.1007/s13296-011-4006-7

International Journal of
STEEL
STRUCTURES
www.springer.com/journal/13296

Behavior of Steel Plate Shear Wall Connected to Frame Beams Only

Lanhui Guo[1]*, Qin Rong[1], Xinbo Ma[2], and Sumei Zhang[1]

[1]*School of Civil Engineering, Harbin Institute of Technology, Harbin, 150090, China*
[2]*Center of Science and Technology of Construction Ministry of Housing and Urban-Rural Development, China*

Abstract

This paper presents the study of steel plate shear walls which are connected to frame beams only. As the shear walls are not connected to frame columns, the premature failure overall buckling or local buckling of frame columns can be prevented. In fact, most of both structural design engineers and architects prefer this kind of steel plate shear walls because the dimension of their opening space is relatively flexible by using several steel plates with small span-to-height ratio placed parallel to each other. In this paper, two steel plate shear walls were fabricated and tested. The influence of stiffeners on the hysteretic behavior of this kind of member was studied. The experimental results showed that this kind of specimen had good ductility and energy dissipation capacity. The energy dissipation capacity of specimen with stiffeners was larger than that of the specimens without stiffeners. Meanwhile, the finite element method was applied to analyze the behavior of steel plate shear walls, whose results were validated by comparing with the corresponding experimental results. Analytical results showed that the free edges deformed with evident out-of-plane deformation and should be constrained by stiffeners to meet the design requirements. The energy dissipation capacity is much better for steel plate shear walls with lower height-to-thickness ratio and larger span-to-height ratio. At last, the skeleton curve of steel plate shear wall was proposed for calculating the elastic rigidity and load-carrying capacity.

Keywords: steel plate shear wall (SPSW), connected to frame beams, ductility, height-to-thickness ratio, span-to-height ratio

1. Introduction

Steel plate shear walls (SPSWs) become popular in steel building structures due to their high lateral strength and stiffness. In the early application of SPSWs, to prevent shear buckling, the wall was stiffened. However, stiffener welding can be costly and time-consuming in steel wall fabrication. In recent years, experimental results indicated that thin-walled steel plates, without stiffeners, perform well in strength and ductility even after the shear buckling occurs. In this context, un-stiffened SPSWs become increasingly popular in the United States and Canada for efficiency and economical purpose. They allow shear buckling and the development of diagonal tension strip occur in these walls which resist the lateral loads by means of the diagonal tension strip action.

Note.-Discussion open until May 1, 2012. This manuscript for this paper was submitted for review and possible publication on December 22, 2010; approved on December 15, 2011.

*Corresponding author
Tel: +86-451-86289100; Fax: +86-451 86289100
E-mail: guolanhui@hit.edu.cn

SPSW is connected to boundary columns and beams either by bolts or welds. The main role of these connections is to transfer shear and tension forces. For SPSWs connected to both frame columns and frame beams, the columns of stiffer system could carry a proportionally larger share of storey shears, which could lead to early failure of column. Xue and Lu (1994) conducted analytical studies on four twelve-storey three-bay system combined with SPSWs. Their results showed that the premature failure of columns can be prevented if shear walls were not connected to frame columns. Thus, the SPSW connected to frame beams only is proposed, in which the steel plate is connected to frame beams by pretensioned high-strength bolts or welds (see Fig. 1). In addition, if this kind of SPSW is fabricated with relatively small span-to-height ratio and is placed parallel to each other in a bay, opening space can be conveniently provided. Therefore, the structural stiffness and load-carrying capacity can be adjusted by changing the size or the number of shear walls, which is welcomed by both structural design engineers and architects.

Since 1980's, un-stiffened steel plate shear walls began to be used in buildings in the United States and Canada. Utilization of the post-buckling strength of a panel in

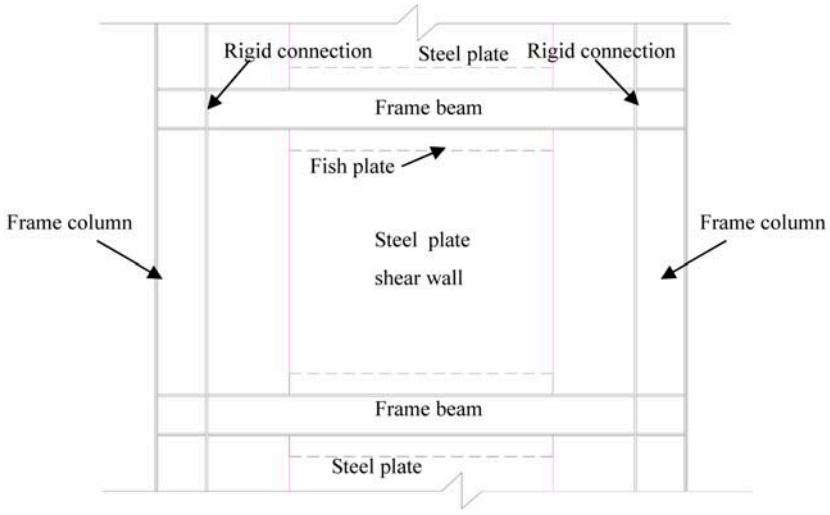

Figure 1. Steel plate shear wall connected to frame beams only.

shear was first applied to steel plate shear wall through a series of analytical and experimental work by Thorburn *et al*. (1983), Timber and Kulak (1983), Tromposch and Kulark (1987). The strip model was proposed and had been adopted by the Canadian Standard CSA-S16-01 as a simple approach for the analysis of unstiffened steel plate shear walls. The concept of post-buckling strength has gained wide attention from researchers in Canada, the United States and England. Elgaaly *et al*. (1993) conducted single layer SPSW tests and proved it could be used as lateral load resisting component. Roberts and Sabouri-Ghomi (1991) carried on a SPSW experiment with holes on the steel panels. All the experiment results showed good ductility and high energy dissipation capacity. Sugii and Yamada (1996), Nakashima *et al*. (1994 and 1995), Driver *et al*. (1997), Lubell *et al*. (2000), Astaneh-Asl and Zhao (2002) studied the behavior of SPSWs in multi-story structures, after that researcher began to focus on the energy dissipation capacity of SPSWs. Behabahanifard *et al*. (2003), Lin and Tsai (2004), and Qu *et al*. (2008) tested the SPSWs and paid more attention on the energy dissipation capacity. Both American code ANSI/AISC 341-05 (2005) and Canadian code CAN/CSA-S16-01 (2001) have provided basic design guides for steel plate shear walls connected to both frame columns and frame beams.

As for SPSWs connected to frame beams, Guo *et al*. (2007) studied the elastic buckling behavior of SPSWs connected to frame beams only using finite element method. In 2009, Xu *et al*. (2009) studied the static behavior of SPSWs connected to frame beams only. Their results showed that this kind of member exhibited good ductility behavior. Until now, there has been few experimental research reported about SPSWs connected to frame beams only, and the hysteretic behavior were not very clear. No guide exists to help the engineers design this kind of SPSW. In this paper, the experiments were carried out and numerical analysis was conducted to investigate the behavior of this kind of SPSW and provide useful information for design.

2. Experiment

2.1. Design and fabrication

Two 1/3 scale SPSWs were fabricated and tested. The frames are single-bay, single-storey with pin-ended beam-to-column connections to ensure the shear wall resists all cyclic horizontal loads. SPSWs are connected to frame beams by four stiffened 125×125×10 mm web angles (see Fig. 2) which are connected to steel plates and frame beams with M20 pretensioned high-strength bolts. The distance between two bolts is 70 mm, as presented in Fig. 2. The steel plate is 1,200 mm high and 1,100 mm long. The effective height of steel plate (distance between the centers of two high-strength bolts along the vertical direction) is 1,100 mm (see Fig. 2). The effective span-to-height ratio L/H is 1.0. The thickness of steel plate is 2.75 mm, and the corresponding height-to-thickness ratio is 400. Table 1 lists the dimension of two specimens. Specimen S1 is not stiffened. Specimen S2 has stiffeners with the dimension of 980×35×2.75 mm welded on free edges (See Fig. 2(b)) to avoid the early buckling of free sides and to study the influence of stiffeners on the hysteretic behavior of the specimens. Three coupons were cut from each steel sheet in accordance with the Chinese standard GB/T 228-2002. Representative stress-strain relationship measured from these tests is shown in Fig. 3, which highlighted the ductile nature of the mild structural steel. The average steel yield stress is 294.7 N/mm^2.

2.2. Experimental setup

The experimental setup is shown in Fig. 4. A hinged frame was installed in the existing loading system, which guaranteed the shear wall only could resist the cyclic

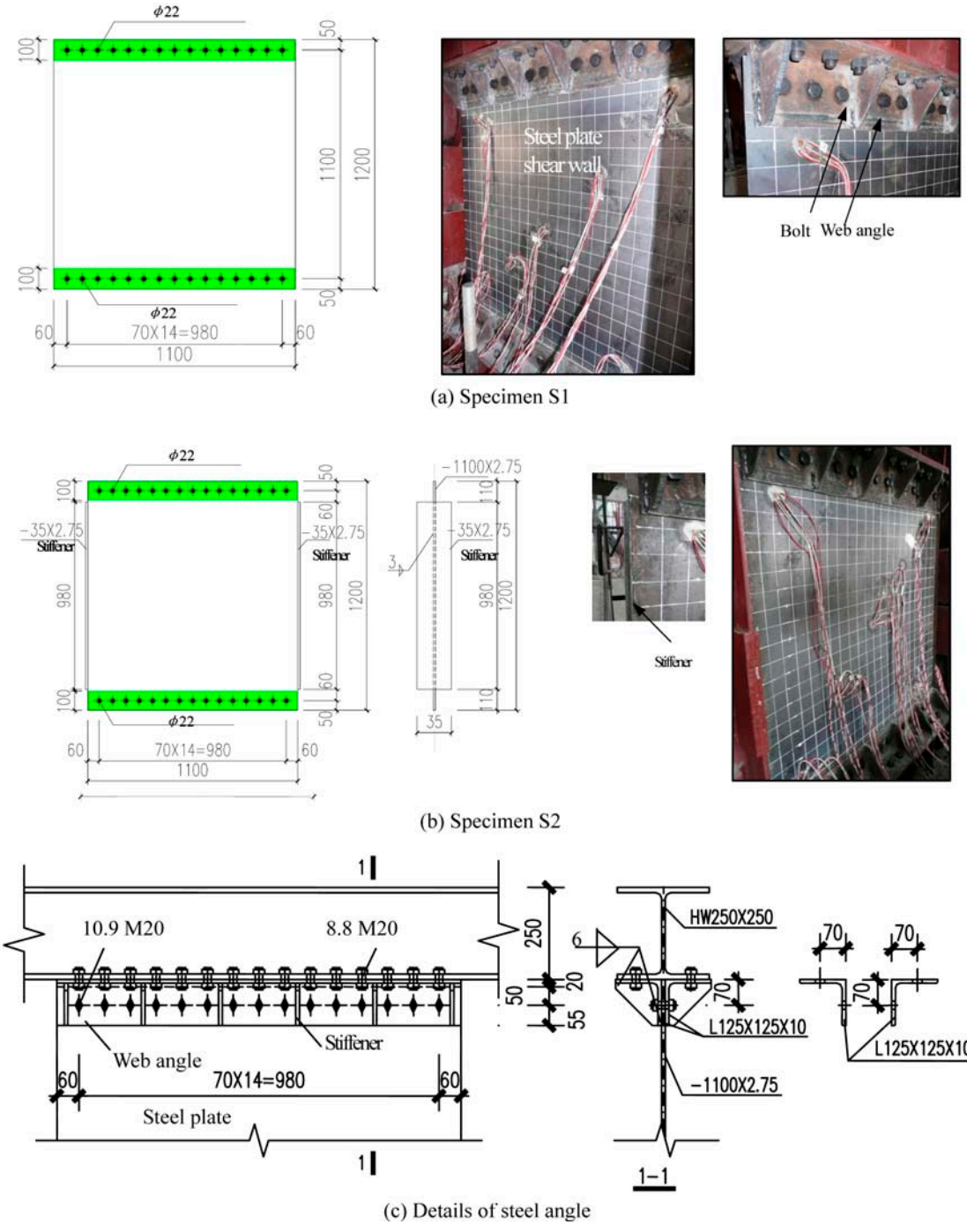

Figure 2. Dimensions of specimen.

Table 1. Dimension and material properties of specimens

No.	Stiffener	H mm	L mm	t mm	λ	t_f mm	b_f mm	f_y N/mm^2	f_u N/mm^2	δ (%)
S1	Without	1100	1100	2.75	400	-	-	294.7	429.9	35.5
S2	With	1100	1100	2.75	400	2.75	35	294.7	429.9	35.5

Note: H is the effective height of SPSW; L is the width of SPSW; t is the thickness of steel plate; λ is the height-to-thickness ratio; t_f is the thickness of stiffener; b_f is the breadth of stiffener; f_y is the steel yield stress; f_u is the steel tensional strength; δ is the elongation ratio.

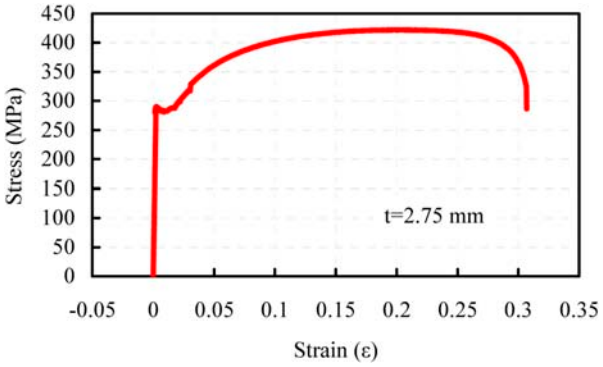

Figure 3. Typical stress-strain relationship curve of steel.

horizontal load induced by an electro-hydraulic servo actuator directly without rotation. The top beam was fixed with the rigid L beam, which was laterally supported at two locations to avoid out-of-plane deformation, and the bottom beam was fixed on the ground. The vertical load (weight of loading system) was designed to be carried by the frame columns. The horizontal displacements were measured by two linear variable displacement transducers (LVDTs) installed on both sides at the top beam. Four LVDTs were installed at the mid-height of steel plate to measure the out-of-plane displacements, whose positions are shown in Fig. 4(b).

The loading method was developed according to the Chinese code JGJ 101-96 (1996). At elastic stage, the horizontal force was regarded as controlling criteria and repeated once at each step. At plastic stage, the horizontal displacement was regarded as controlling criteria and repeated twice at each step.

3. Experimental Results and Analysis

Specimen S1 is a SPSW without stiffeners. When the load reached 39% of load-carrying capacity, the corresponding drift ratio was 0.2%. The drift ratio is equal to the horizontal displacement divided by the effective height of steel plate. At this time, the out-of-plane buckling started at the corner of steel plate due to its compressive stress state. With the increase of load, the buckling at corner became more pronounced. When the load reached 160 kN (77% of load-carrying capacity), the tension field along the diagonal direction appeared as shown in Fig. 5(a). As a consequence of this buckling waves appeared on the plate. As the loading direction changed, the buckling waves changed accordingly with pinging sound. Despite of the change in buckling wave directions, the out-of-plane buckling direction remained unchanged. When the drift ratio reached 0.24%, the corresponding out-of-plane deformation was 26.7 mm. The area under the hysteretic

(a)

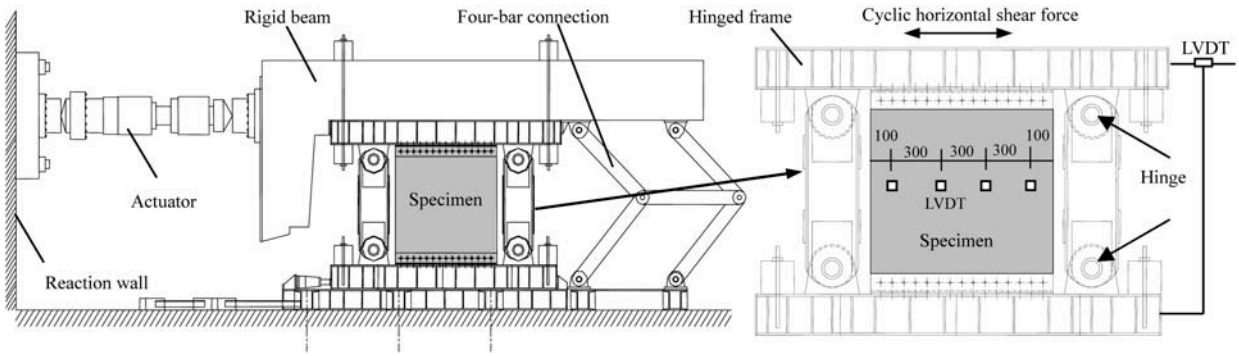

(b)

Figure 4. Experimental setup.

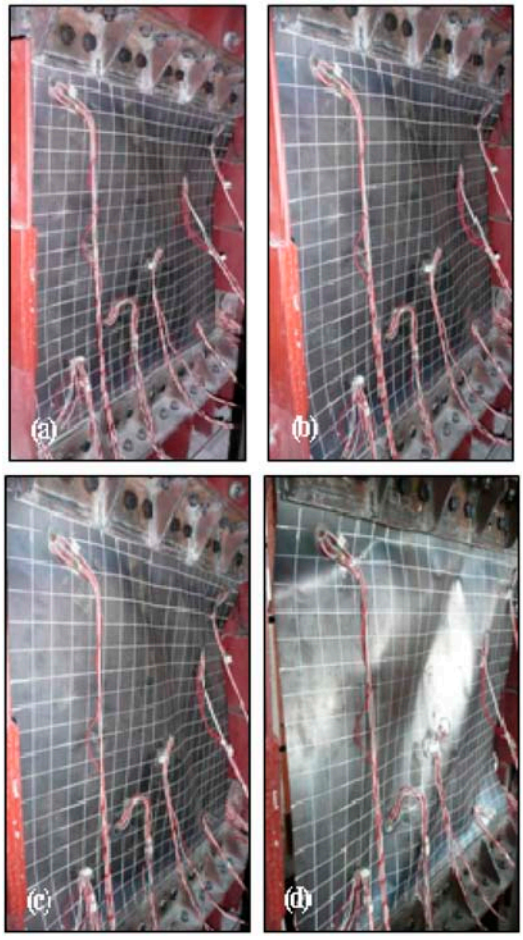

Figure 5. Experimental phenomena of specimen S1.

curve was small, indicating that the energy dissipation capacity was low at this stage. When the drift ratio reached 1.1% (horizontal displacement of 12 mm), the rigidity decreased evidently. The out-of-plane deformation developed dramatically, as shown in Fig. 5(b). At this point, the pinching effect of hysteretic curves appeared due to the out-of-plane buckling of SPSWs. Two diagonal tension strips appeared when the drift ratio reached 1.5% (see Fig. 5(c), horizontal displacement of 16 mm), and the corresponding out-of-plane deformation was 36 mm. The ultimate load-carrying capacity of 206.9 kN (-202.4 kN) was reached with the corresponding drift ratio of 1.8% (–1.7%) (horizontal displacement of 19.5 mm (–18.6 mm)), whose phenomenon is shown in Fig. 5(d). After that, the load decreased slightly with the increase of horizontal displacement. When the drift ratio reached 3.6% (horizontal displacement of 40 mm), the load decreased by 7.8% of the load-carrying capacity, indicating good ductility behavior of SPSW connected to frame beams. At this stage, the maximum range of LVDT was reached and the test was stopped. The hysteretic curve of specimen S1 is shown in Fig. 6.

Comparing with specimen S1, specimen S2 exhibited no evident phenomenon at the plate corner before the

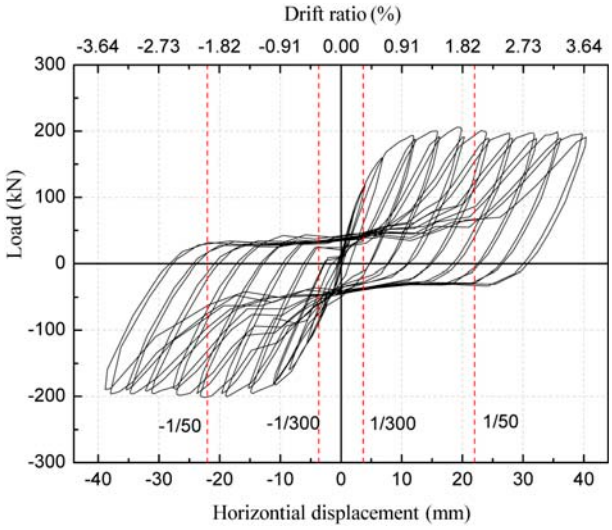

Figure 6. Load-drift ratio (horizontal displacement) reaction curve of specimen S1.

load reached 39% of load-carrying capacity (drift ratio of 0.2%). The reason was that the stiffeners stiffened the steel plate to avoid the early buckling of free sides. The tension strip along diagonal direction appeared when the load reached 160 kN (horizontal displacement of 7.1 mm, drift ratio of 1/150), as shown in Fig. 7(a). With the change of loading direction, the direction of tension strip changed accompanying with pinging sound. The hysteretic curve appeared pinching effect because of buckling of steel plate. When the drift ratio reached 1.1% (horizontal displacement of 12 mm), the specimen was in elastic-plastic stage, and the stiffener appeared out-of-plane deformation (see Fig. 7(c)). But the out-of-plane deformation of steel plate near the stiffeners was evidently smaller than that of specimen S1 with the same loading level. The ultimate load-carrying capacity of 208.5 kN (–199.6 kN) was reached with the corresponding drift ratio of 1.4% (–1.7%) (horizontal displacement of 15.7 mm (–18.9 mm)). After then, the load decreased slowly with the increase of drift ratio. When the drift ratio reached 3.6% (horizontal displacement of 40 mm), the stiffeners appeared evident out-of-plane deformation and the test was stopped. The experimental phenomenon is shown in Fig. 7. The load-horizontal displacement reaction curve is shown in Fig. 8.

According to the Chinese Code for Seismic Design of Building (GB 50011-2010), the steel structures should remain in elastic stage before the maximum storey drift ratio reaches 1/300 under small seismic events. The maximum storey drift ratio should reach 1/50 under severe seismic events. Under wind load, the maximum storey drift ratio should be less than 1/500. From the test of specimen S1 and S2 (see Fig. 6 and Fig. 8), it can be found that those two specimens remain elastic when the storey drift ratio was smaller than 1/300. The maximum storey drift ratio of SPSW was still over 1/50. It can be concluded that this kind of SPSW can be used in the

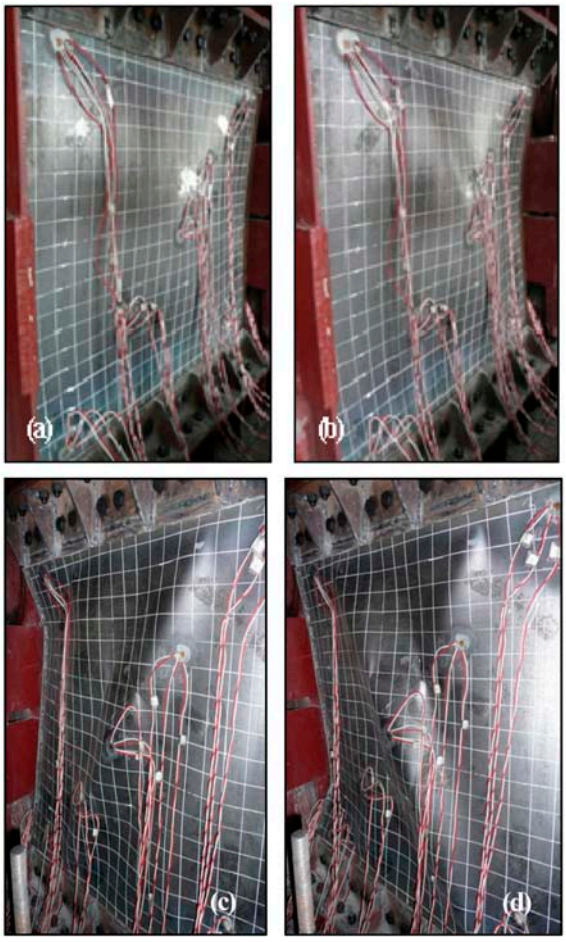

Figure 7. Experimental phenomena of specimen S2.

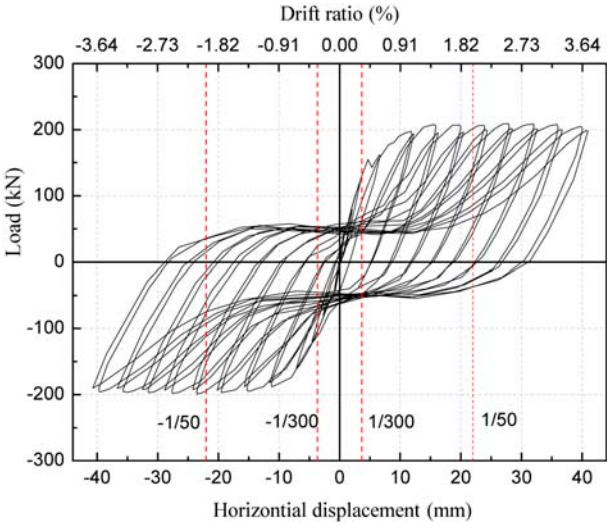

Figure 8. Load-drift ratio (horizontal displacement) reaction curve of specimen S2.

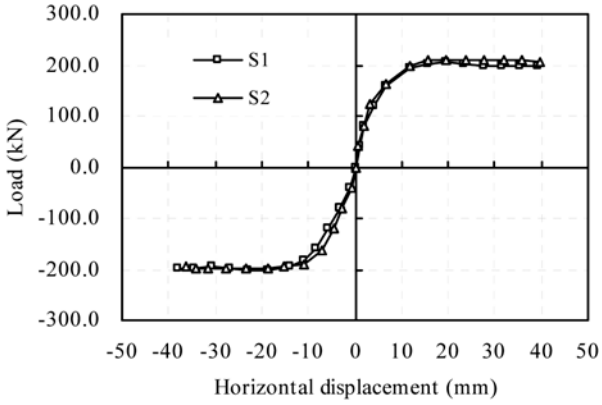

Figure 9. Comparison of skeleton curves.

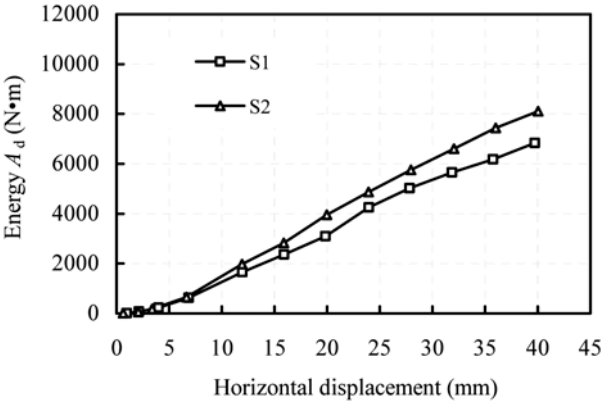

Figure 10. Comparison of absorbed energy.

structural system as a kind of earthquake resistance members or wind load resistance members.

For specimen S1 and S2, the main difference was that the stiffeners were welded on specimen S2. The comparison of skeleton curves is shown in Fig. 9. It can be seen that the stiffeners had a little influence on load-carrying capacity and ductility of SPSWs. The reason was that the tension strip appeared to resist the lateral load in plastic stage, and the stiffeners had no evident influence on the occurrence of tension strips. Absorbed energy and energy dissipation ratio are two important indexes to evaluate seismic behavior of SPSWs. The former expresses how much energy is absorbed in each loading step. The latter is the efficiency of energy dissipation capacity. The area of hysteretic curve A_d denotes the absorbed energy in each loading step. With larger area, the specimen possesses higher energy dissipation capacity and good earthquake resistance. Figure 10 presents the difference of hysteretic curve areas for these two specimens under different horizontal displacements. It can be seen that there was no evident difference when the horizontal displacement was less than 6.7 mm (drift ratio of 0.6%). After then, the energy dissipation capacity of specimen S2 was higher than that of specimen S1. When the horizontal displacement reached 40 mm (drift ratio of 3.6%), the area of specimen S2 was 36% larger than that of specimen S1. It can be seen that the stiffeners decreased the pinching effects of hysteretic curve, thus increased the energy dissipation capacity of SPSW effectively. The energy dissipation ratio can be calculated according to Equation (1), in

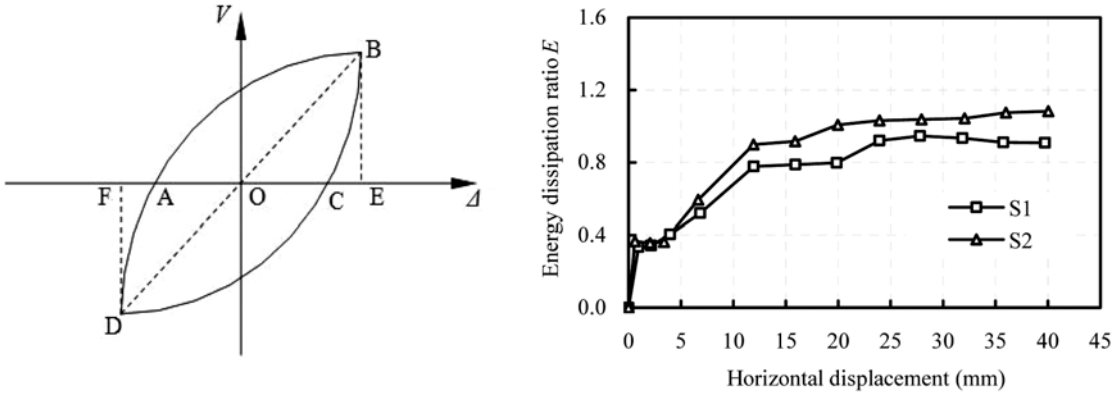

(a) Energy dissipation ratio (b) Comparison of energy dissipation ratios

Figure 11. Comparison of energy dissipation capacity of SPSWs.

which S denotes area, and all area symbols are shown in Fig. 11(a). Figure 11(b) shows the comparison of energy dissipation ratios. It can be seen that the energy dissipation ratio of specimen S2 was higher than that of specimen S1 when the horizontal displacement was over 3.9 mm. The reason was that the function of stiffeners increases the energy dissipation ratio of SPSWs.

$$E=\frac{S_{ABC}+S_{CDA}}{S_{OBE}+S_{ODF}} \tag{1}$$

4. Numerical Analysis

4.1. Finite element model

Finite element software *ANSYS* is used to analyze the behavior of SPSW under cyclic load. In the analysis, yield and post-buckling behavior of steel plate is considered. The beam element BEAM189 is used to analyze the behavior of frame beams and frame columns. The shell element SHELL181 is used to model the behavior of SPSWs and stiffeners. An imperfection assigned as the first order buckling mode has been introduced in the finite element model. The amplitude of the imperfection is 1/1000 length of SPSW. The finite element model is shown in Fig. 12. The load was applied at the top of frame beam by increasing horizontal displacement.

Material properties specified in *ANSYS* include the modulus of elasticity of steel E_s of 2.0×10^5 MPa and the Poisson's ratio v_s of 0.3. The steel is assumed to behave as an elastic-plastic material. The idealized stress-strain relationship curve used in the analysis is shown in Fig. 13. Figure 14 shows the comparison of hysteretic curves between numerical and experimental results. It can be seen that they agreed well with each other. The finite element model can be well used to model the behavior of SPSWs under cyclic load.

4.2. Analysis of SPSWs

In the following analysis, common parameters are shared such as the dimension of beams and columns. The

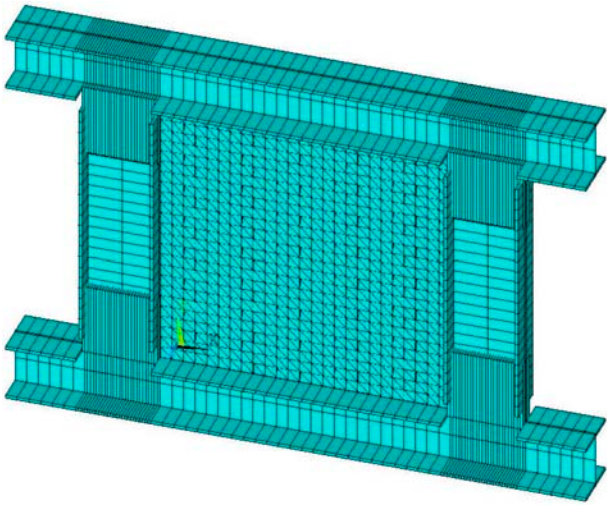

Figure 12. Finite element model.

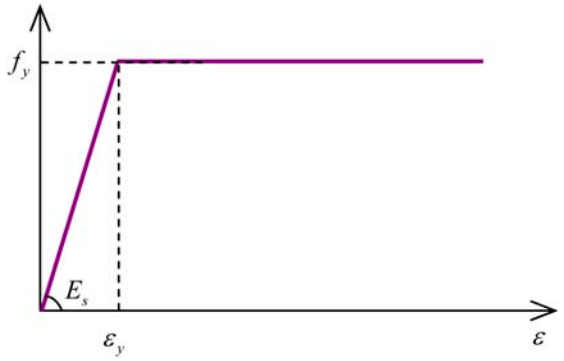

Figure 13. Typical stress-strain relationship of steel.

profiled steel H420×350×15×20 mm is selected as column. The names of Chinese designation H shapes reflect their depth, flange width, as well as web and flange thicknesses. And two rigid frame beams are selected with a 500×500 mm square solid cross section. The steel with yield stress of 345 N/mm^2 for both frame and steel plate wall is adopted. Story height is a constant value of 1800 mm and span L varies from 900 mm to 4500 mm to change the

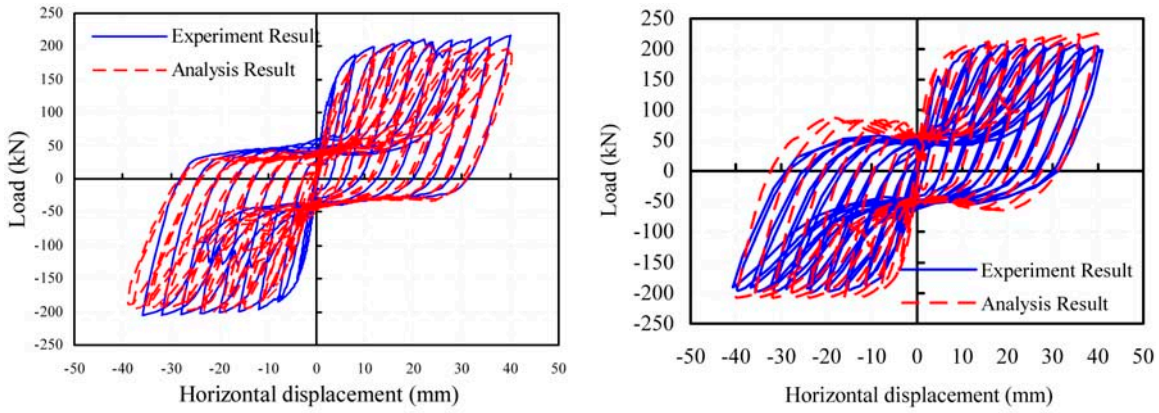

Figure 14. Comparison between experimental and analytical results.

Table 2. Span-to-height ratio and span length

Span-to-height ratio β	0.5	1.0	1.5	2.0	2.5
Span (mm)	900	1800	2700	3600	4500

span-to-height ratio. Height-to-thickness ratio λ follows the variation of the thickness t which varies from 100 to 500. In the analysis, there is no stiffener on the free side. The span-to-height ratio and height-to-thickness ratio are summarized in Table 2 and Table 3 respectively.

The finite element models are developed and analyzed, and the average shear stress-horizontal displacement relationship curves are presented in Fig. 15. The average shear stress is equal to shear force divided by the area of SPSW ($A=L\times t$). These curves are chosen to easily estimate the stress state of steel plate. It can be seen that the height-to-thickness ratio has considerable influence on the cyclic behavior of SPSWs. When the height-to-thickness ratio is small, the SPSW exhibits plump hysteretic curve under cyclic loading, meaning better energy dissipation capacity. With the increase of height-to-thickness ratio, the pinch effect of hysteretic curves becomes more severe, and the maximum shear stress decreases gradually. The reason is that the out-of-plane deformation developes quickly with the increase of height-to-thickness ratio. With the increasing of span-to-height ratio, the ultimate shear stress increases evidently. All curves show no dropping trend illustrating that this component has good ductility behavior.

Table 4 summarizes the ultimate shear stress of SPSWs, from which more information can be derived. The ultimate shear stress is lower than shear yield stress $345/\sqrt{3}$ MPa. When the height-to-thickness ratio is over 200, the ultimate shear stress decreases considerably with the increase of height-to-thickness ratio.

Table 4. Ultimate shear stress (MPa)

	β=0.5	β=1.0	β=1.5	β=2.0	β=2.5
λ=100	69	111	122	135	137
λ=150	56	102	114	130	134
λ=200	53	86	111	122	134
λ=250	52	82	109	122	131
λ=300	51	86	108	122	130
λ=400	50	84	105	120	130
λ=500	50	83	100	117	128

Figure 16 shows the out-of-plane deformation at the drift ratio of 2%. Table 5 summarizes the maximum value of out-of-plane deformation. Because the steel plates are not connected to frame columns, the free edges appear bigger out-of-plane deformation than the inner buckle wave. With the increase of span-to-height ratio, more half-waves form due to the increased length of SPSWs. With the increase of height-to-thickness ratio, the numbers of half-wave increase but the amplitude of each half-wave decreases. Thinner plates buckle more easily and more tension strips appear. This reduces the out-of-plane deformation. The maximum out-of-plane deformation also decreases gradually with the increasing of height-to-thickness ratio. The reason is that more buckling waves appear with the increasing of lateral displacement.

The out-of-plane deformation shows that even thin plates tend to develop tension strip to resist the lateral load. Compared to SPSWs connected to both frame beams and frame columns, SPSWs connected to beams only appears less tension strips as only beams can provide anchor boundary condition. In this context, the SPSW connected to two sides lost certain lateral load resisting

Table 3. Height-to-thickness ratio and panel thickness

Height-to-thickness ratio λ	100	150	200	250	300	400	500
Thickness t (mm)	18	12	9	7.2	6	4.5	3.6

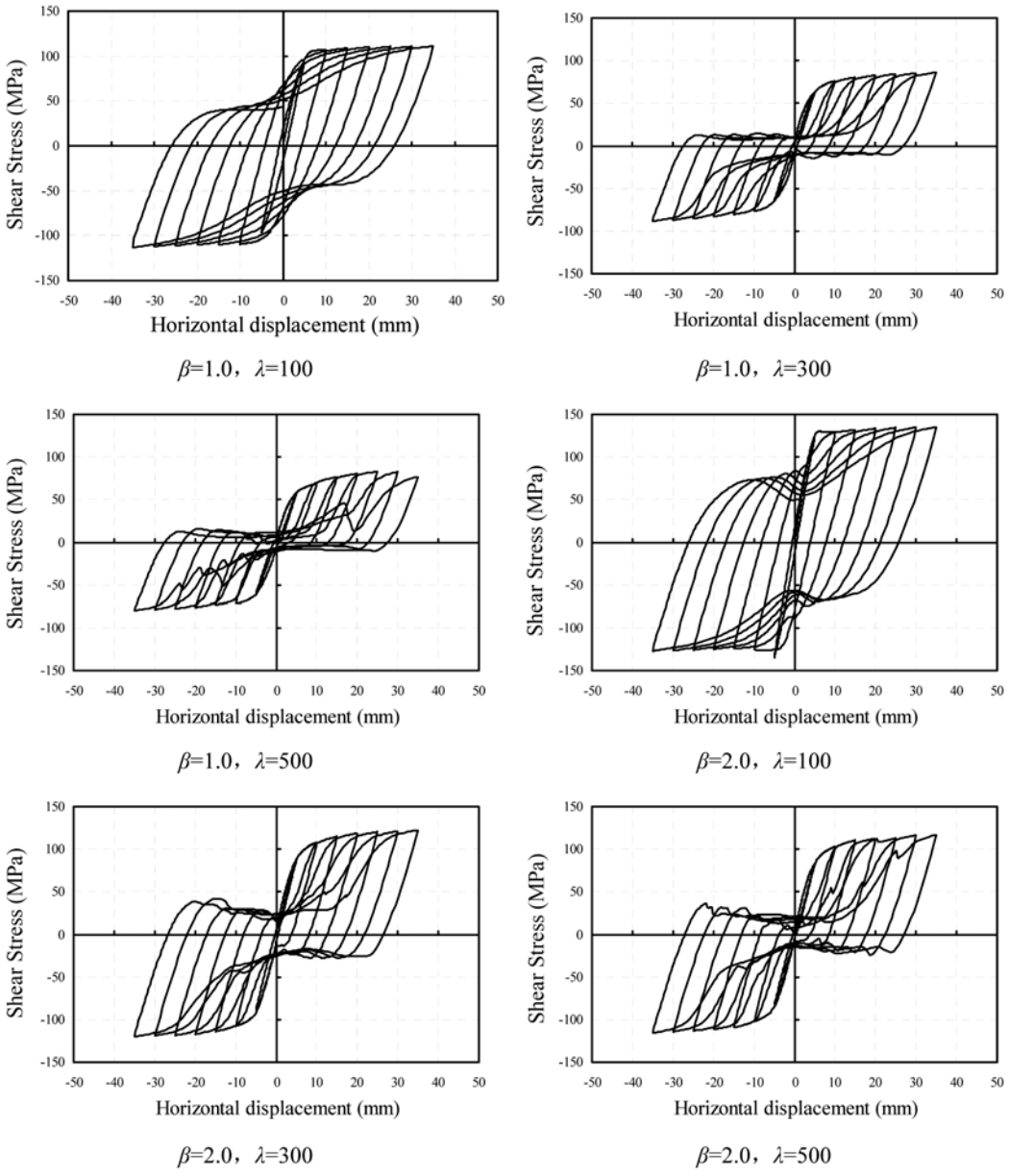

Figure 15. Hysteretic curves of steel plate shear wall.

ability, but the columns in them are also free of extra load induced by constraining steel plates. In this case, the span-to-height ratio considerably affects the mechanical behavior of this kind of members because the number of tension strips depends on this ratio. Figure 17 shows the principal stress trace which reveals more details about the tension strips.

Span-to-height ratio of 1.0 seems to be the boundary line which divides the mechanism of SPSWs into two situations. Plate with small span-to-height ratio is difficult to form tension strip, so the load-carrying capacity and energy dissipation ratio stay in a low level. When the span-to-height ratio is less than 1, the panel with small height-to-thickness ratio just buckles on the two free edges and no tension strips occurs. When the height-to-thickness ratio increases over 1, thin plates buckle easily and tension strips form eventually. Steel plates with higher span-to-height ratio are more prone to develop tension strips and can resist higher lateral load. In general, stiff boundary is necessary for tension strips when the strips can exhibit the best lateral load resisting ability. These two points above explain the mechanism of SPSWs connected to frame beams only. The principal stress trace figures and hysteretic curves show two rules in the use of this kind of SPSWs. When span-to-height ratio is less than 1, thicker plate is recommended, stiffeners such as ribs, and square tubes are suggested for free edges. For SPSWs with thin plate, larger span-to-height ratio is more economical.

Excellent energy dissipation capacity is one of main

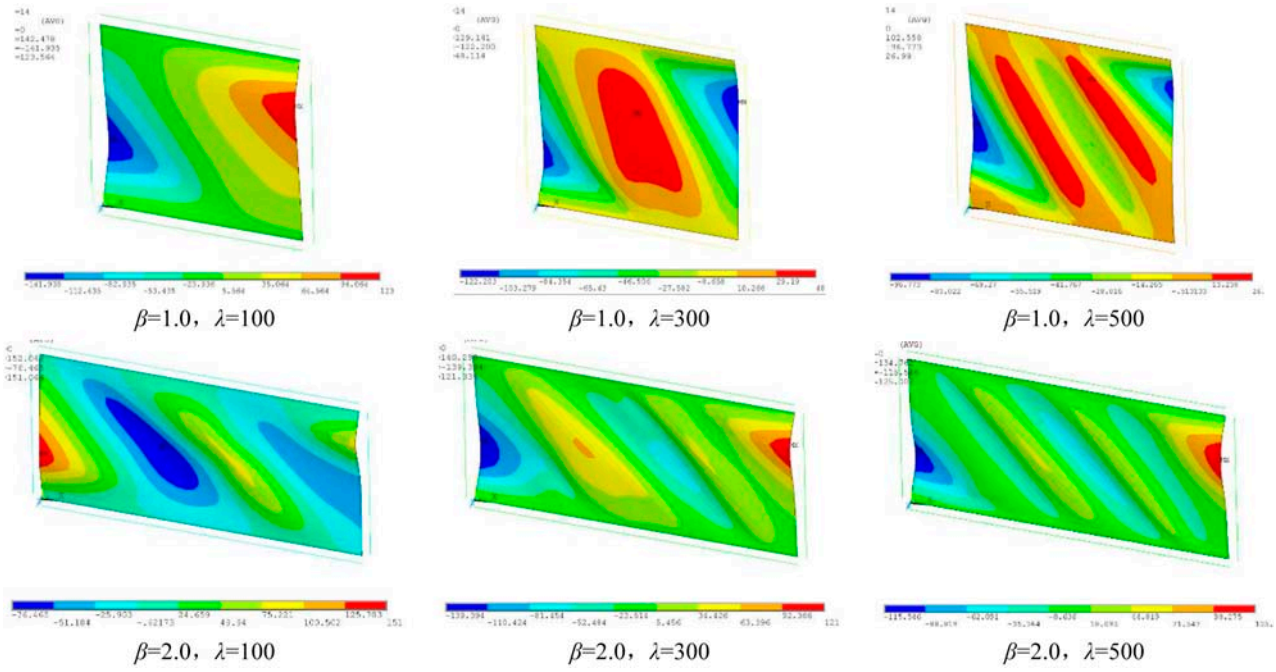

Figure 16. Out-of-plane deformation of SPSW.

Table 5. Maximum out-of-plane deformation (mm)

	β=0.5	β=1.0	β=1.5	β=2.0	β=2.5
λ=100	102	142	144	151	137
λ=150	102	132	141	151	149
λ=200	100	119	138	145	150
λ=250	96	120	135	144	146
λ=300	94	122	132	140	138
λ=400	87	110	117	121	121
λ=500	80	97	114	125	122

advantages of SPSWs. Figure 18 shows the variation of loop area. The dissipated energy of different models has similar tendency. This index varies linearly from nearly zero to a high level, and lower initial value means SPSWs stay in an elastic status under low lateral load. This means SPSWs system could provide high initial stiffness. The nearly straight climbing lines display excellent performance of SPSWs. Of course, thicker plate can absorb more energy.

Figure 19 shows the variation of energy dissipation

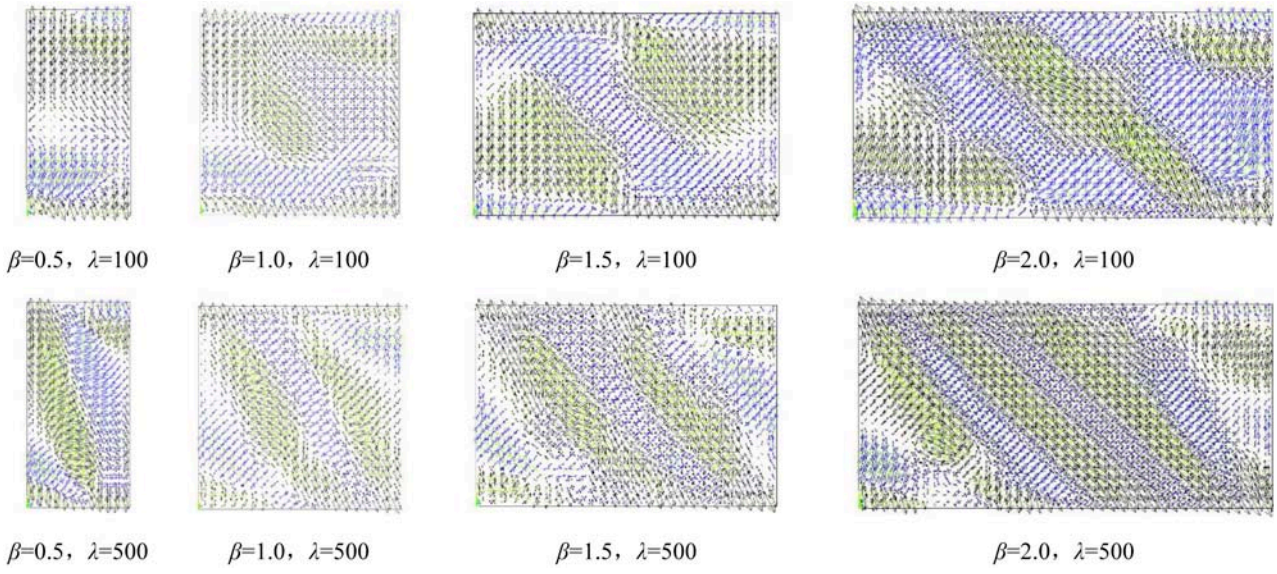

Figure 17. Principle stress trace distribution.

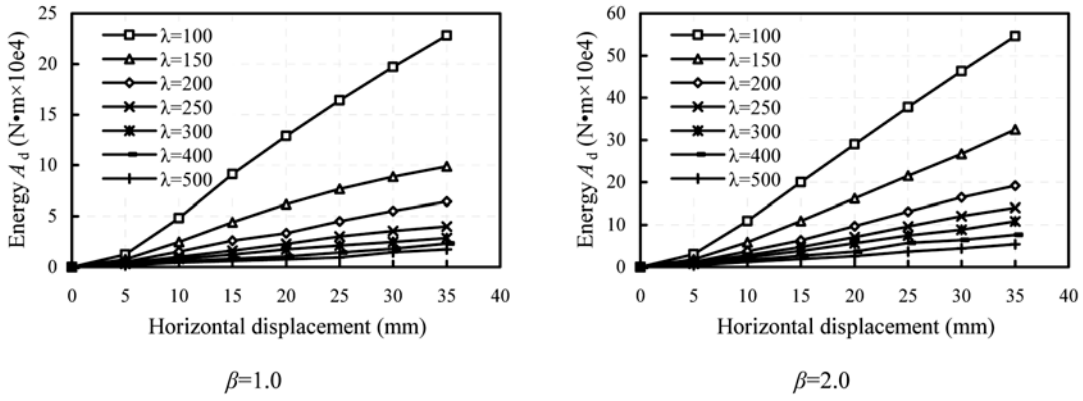

Figure 18. Loop area of each step.

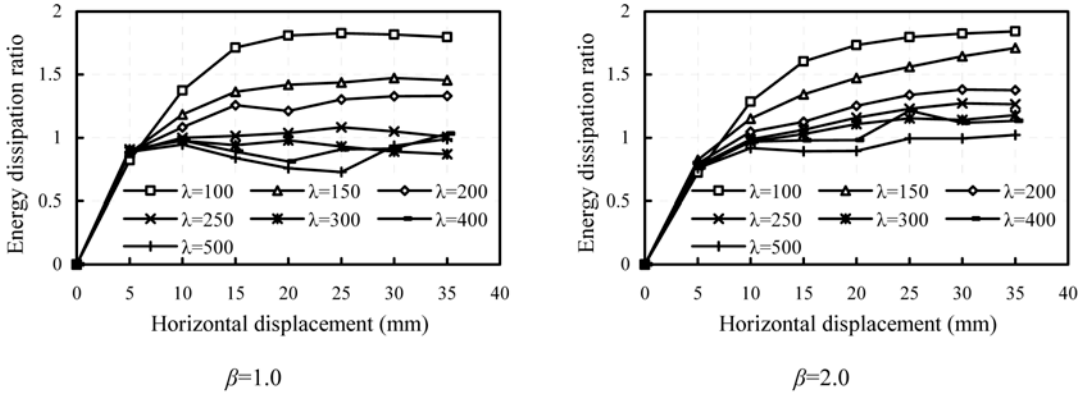

Figure 19. Energy dissipation ratio at each step.

ratio. Along with the increasing of lateral displacement, energy dissipation ratio first increases rapidly and then stays at nearly a constant value. This shows stable energy dissipation capacity under severe lateral load. This excellent characteristic shows that although SPSWs have severe pinch effect, the huge energy consuming ability makes it being a good component under earthquake. When the height-to-thickness ratio is less than 250, the energy dissipation ratio of SPSWs can reach a relative high level because thick plates don't buckle as severe as thin plates, and this ensures the plates behave in a better way. But when the height-to-thickness ratio is over 250, severe out-of-plane deformation develops. The span-to-height ratio also affects the energy dissipation ratio, because the large span-to-height ratio ensures the tension fields develop easily. More tension strips means better energy dissipation capacity. In this point, plates with small span-to-height ratios and thick plates would provide better results. While for thin plate, the large span-to-height ratio is proposed.

5. Simplified Skeleton Curve of SPSWs

According to the average shear stress-horizontal displacement relationship curves, it is assumed that the shear force V-horizontal displacement Δx skeleton curve is elastic and perfectly plastic as shown in Fig. 20, where

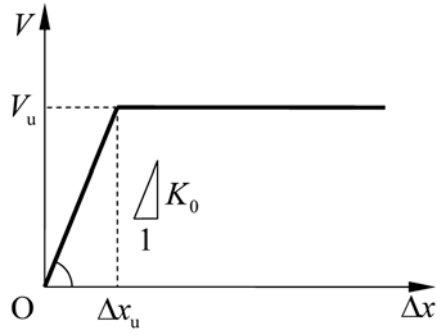

Figure 20. Simplified model of V-Δx skeleton curve.

K_0 is the stiffness of elasticity and V_u is the ultimate load-carrying capacity of SPSWs.

5.1. Stiffness of elasticity

The SPSW can be idealized as a member fixed at both two bottoms, for which the frame beams act as the fixed ends. In general, it is necessary to consider both the shear and overall bending deformations of the shear wall in structure mechanics analysis.

The member with height H and length L is fixed at two ends and is subjected to a horizontal force V as shown in Fig. 21. The total displacement Δx can be expressed as

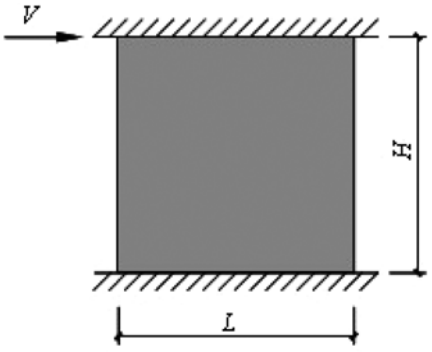

Figure 21. SPSW connected to frame beams only.

$$\Delta x=\Delta x_M+\Delta x_V \tag{2}$$

where Δx_M and Δx_V denote bending deformation and shear deformation, respectively. Using the Graph Multiplication Method in Structure Mechanics, the bending deformation Δx_M and shear deformation Δx_V can be determined as follows,

$$\Delta x_M=\frac{VH^3}{12E_sI}=\frac{V}{E_st(L/H)^3} \tag{3}$$

$$\Delta x_V=\frac{kVH}{G_sA}=\frac{2(1+v_s)\cdot kV}{E_st(L/H)} \tag{4}$$

where E_sI is the overall bending stiffness, G_sA is the shear stiffness, t denotes the thickness of steel plate, v_s is the Poisson's ratio and k is the correction coefficient considering non-uniform shear stress distribution on the cross-section. For rectangular cross-section, k is equal to 1.2.

Substituting Eqs. (3) and (4) to Eq. (2), the value of Δx is defined by the following equation

$$\Delta x=\frac{V}{E_st}\left[\frac{1}{(L/H)^3}+\frac{2(1+v_s)\cdot k}{(L/H)}\right] \tag{5}$$

In the elastic stage, the shear force V is proportional to the horizontal displacement Δx, i.e.

$$V=K_0\cdot\Delta x \tag{6}$$

Substituting Eq. (6) to Eq. (5) gives

$$K_0=\frac{E_st}{1/(L/H)^3+2(1+v_s)\cdot k/(L/H)} \tag{7}$$

From known dimensions and material properties of SPSW, the elastic stiffness K_0 of SPSW can be determined.

5.2. Ultimate load-carrying capacity

The finite element method was used to study the influence of height-to-thickness ratio and length-to-height ratio on the behavior of SPSWs under cyclic load. The ultimate shear stress of SPSW is presented in Table 4. Based on the analysis results, the approximate simulated formula for calculating ultimate load-carrying capacity can be fitted:

$$V_u=[0.23\ln(L/H)-0.13\ln(\lambda)+1.22]\cdot f_vLt \tag{8}$$

where λ denotes the height-to-thickness ratio of SPSW and f_v denotes the shear yield stress of steel.

6. Conclusions

This paper presented the study of SPSWs connected to frame beams only. The experimental results illustrated that the steel plate possessed good ductility and excellent energy dissipation capacity. The stiffeners on free edges increased the energy dissipation capacity, but had no evident influence on the load-carrying capacity and ductility of the members. The numerical results are validated by comparing with the corresponding experimental results. The influence of height-to-thickness ratio and span-to-height ratio on hysteretic behavior of this kind of members is analyzed. The results show that both the height-to-thickness ratio and the span-to-height ratio considerably affect the hysteretic behavior of SPSWs. Specimen with low height-to-thickness ratio has plump hysteric curves under cyclic loading indicating its excellent energy absorbing capability. When the span-to-height ratio is larger than 1.0, more tension strips appear to resist the lateral load. If the span-to-height ratio is less than 1.0, the tension fields can not be fully developed and results in decrease of load-carrying capacity. The skeleton curve was proposed for practical application, and it can be noted that the proposed skeleton curve predicts elastic rigidity and load-carrying capacity of SPSWs satisfactorily.

Acknowledgment

The project is supported by National Natural Science Foundation of China (No. 50808053), Natural Science Foundation of Heilongjiang Province of China (ZJG0701), which are gratefully acknowledged.

References

AISC (2005). *Seismic provisions for structural steel buildings*. ANSI/AISC 341-05, American institute of steel construction, Chicago, IL.

Astaneh-Asl, A. and Zhao, Q. (2002). "Cyclic behavior of steel shear wall systems." *Proc. Annual Stability Conference*, Structural Stability Research Council, Seattle.

Behbahanifard, M. R., Grondin, G. Y., and Elwi, A. E. (2003). *Experimental and numerical investigation of steel plate shear wall*. Structural Engineering Report 254, University of Alberta, Canada.

CAN/CSA S16-01 (2001). *Limit states design of steel*

structures. Canadian standards association, Willowdale, Ontario, Canada.

Driver, R. G., Kulak, G. L., Kennedy, D. J. L., and Elwi, A. E. (1997). *Seismic behavior of steel plate shear walls*. Structural Engineering Report 215, University of Alberta, Canada.

Elgaaly, M., Caccese, V., and Martin, D. K. (1993). *Experimental investigation of the behavior of bolted thin steel plate shear walls*. Civil Engineering Department, University of Maine, Orono, Maine.

GB/T 228-2002 (2002). *Metallic materials-Tensile testing at ambient temperature*. General Administration of Quality Supervision, Inspection and Quarantine of the People's Republic of China, Beijing, China (in Chinese).

GB 50011-2010 (2010). *Code for seismic design of buildings*. Ministry of Housing and Urban-Rural Development of the people's Republic of China, Beijing, China (in Chinese).

Guo, Y., Miu, Y., and Dong, Q. (2007). "Elastic buckling behavior of stiffened steel plate shear walls slotted at two edges." *Progress in Steel Building Structures*, 9(3), pp. 58-62 (in Chinese).

JGJ 101-96 (1996). *Specification of testing methods for earthquake resistant building.* Ministry of Construction of the people's Republic of China, Beijing, China (in Chinese).

Lin, Y. C. and Tsai, K. C. (2004). *Seismic response of steel shear wall constructed with restrains*. Technical Report NCREE-04-015, National Center for Research on Earthquake Engineering, Taipei, Taiwan (in Chinese).

Lubell, A., Prion, H., Ventura, C., and Rezai, M. (2000). "Unstiffened steel plate shear wall performance under cyclic loading." *Journal of Structural Engineering*, ASCE, 126(4), pp. 453-460.

Nakashima, M., Akawaza, T., and Tsuji, B. (1995). "Strain-hardening behavior of shear panels made of low-yield steel. II: Model." *Journal of Structural Engineering*, ASCE, 121(12), pp. 1750-1757.

Nakashima, M., Iwai, S., Iwata, M., Takeuchi, T., Konomi, S., Akazama, T., and Suburi, K. (1994). "Energy dissipation behavior of shear panels made of low yield steel." *Earthquake Engineering and Structural Dynamics*, 23, pp. 1299-1313.

Qu, B., Bruneau, M., Lin, C. H., and Tsai, K. C. (2008). "Testing of full-scale two-story steel plate shear wall with reduced beam section connections and composite floors." *Journal of Structural Engineering*, 134(3), pp. 364-373.

Roberts, T. and Sabouri-Ghomi, S. (1991). "Hysteretic characteristics of unstiffened plate shear panels." *Thin Walled Structures*. 12(2), pp. 145-162.

Sugii, K., and Yamada, M. (1996). "Steel panel shear salls with and without concrete covering." *Proc. on CD-Rom, 11th World Conference on Earthquake Engineering,* Acapulco, Mexico, Paper No. 403.

Thorburn, L. J., Kulak, G. L., and Montgomery, C. J. (1983). *Analysis of steel plate shear walls*. Structural Engineering Report No. 107, Department of Civil Engineering, University of Alberta, Edmonton, Canada.

Timber, P. A. and Kulak, G. L. (1983). *Experimental study of steel plate shear walls.* Structural Engineering Report No. 114, University of Alberta, Canada.

Tromposch, E. W. and Kulak, G. L. (1987). *Cyclic and static behaviour of thin panel steel plate shear walls*. Structural Engineering Report No. 145, University of Alberta, Canada.

Xue, M. and Lu, L. W. (1994). "Monotonic and cyclic behavior of infilled steel shear panels." *Proc. 17th Czech and Slovak International Conference on Steel Structures and Bridges*, Bratislava, Slovakia.

Xu, M., Wang, Y., and Zhang, S. (2009). "Shear resistance behavior of two-side connected steel-plate shear wall (SPSW)." *Industrial Construction*, 39(3), pp. 107-111 (in Chinese).